COMPUTATIONAL
ANDSTRUCTURAL
BIOTECHNOLOGY
JOURNAL

Dependence of SARS-CoV-2 infection on cholesterol-rich lipid raft and endosomal acidification

Xiaowei Li [a,b,c,1], Wenhua Zhu [b,c,1], Meiyang Fan [b,c], Jing Zhang [b,c], Yizhao Peng [b,c], Fumeng Huang [b,c], Nan Wang [d], Langchong He [d], Lei Zhang [e], Rikard Holmdahl [a,b,c,f], Liesu Meng [a,b,c,*], Shemin Lu [a,b,c,*]

[a] National Joint Engineering Research Center of Biodiagnostics and Biotherapy, Second Affiliated Hospital, Xi'an Jiaotong University, 710004 Xi'an, China
[b] Institute of Molecular and Translational Medicine (IMTM), and Department of Biochemistry and Molecular Biology, School of Basic Medical Sciences, Xi'an Jiaotong University Health Science Center, 710061 Xi'an, China
[c] Key Laboratory of Environment and Genes Related to Diseases (Xi'an Jiaotong University), Ministry of Education of China, 710061 Xi'an, China
[d] School of Pharmacy, Xi'an Jiaotong University, 710061 Xi'an, China
[e] Shaanxi Provincial Centre for Disease Control and Prevention, 710054 Xi'an, China
[f] Section for Medical Inflammation Research, Department of Medical Biochemistry and Biophysics, Karolinska Institute, Stockholm 171 77, Sweden

ARTICLE INFO

ABSTRACT

Coronavirus disease 2019 is a kind of viral pneumonia caused by severe acute respiratory syndrome coronavirus 2 (SARS-CoV-2). However, the mechanism whereby SARS-CoV-2 invades host cells remains poorly understood. Here we used SARS-CoV-2 pseudoviruses to infect human angiotensin-converting enzyme 2 (ACE2) expressing HEK293T cells and evaluated virus infection. We confirmed that SARS-CoV-2 entry was dependent on ACE2 and sensitive to pH of endosome/lysosome in HEK293T cells. The infection of SARS-CoV-2 pseudoviruses is independent of dynamin, clathrin, caveolin and endophilin A2, as well as macropinocytosis. Instead, we found that the infection of SARS-CoV-2 pseudoviruses was cholesterol-rich lipid raft dependent. Cholesterol depletion of cell membranes with methyl-β-cyclodextrin resulted in reduction of pseudovirus infection. The infection of SARS-CoV-2 pseudoviruses resumed with cholesterol supplementation. Together, cholesterol-rich lipid rafts, and endosomal acidification, are key steps of SARS-CoV-2 required for infection of host cells. Therefore, our finding expands the understanding of SARS-CoV-2 entry mechanism and provides a new anti-SARS-CoV-2 strategy.

1. Introduction

Coronavirus disease 2019 (COVID-19), which is caused by the severe acute respiratory syndrome coronavirus 2 (SARS-CoV-2), has rapidly increased in epidemic scale of the world since its initial outbreak during the winter of 2019 [1,2]. Up to march 2021 the number of confirmed cases worldwide exceeds 100 million, with more than 2.15 million deaths. This pandemic is of international concern and subject to intense investigations and many pathological features of COVID-19 have yet to be characterized.

To enter the host cells, viruses specifically interact with a membrane component and subsequently integrate in the cell membrane to release the genome into the cytosol, or alternatively take advantage of the endocytic pathway [3,4]. The cellular entry of SARS-CoV-2 has been shown to be facilitated by the serine protease transmembrane protease serine 2 (TMPRSS2) for spike (S) protein priming [5]. Moreover, Hoffmann et al. [5] and Zhu et al. [6] found that SARS-CoV-2 preferentially enters cells through the plasma membrane fusion pathway in Calu-3 cells expressing the TMPRSS2, whereas SARS-CoV-2 enters via endosomal pathway in HEK293T and Vero cells that express no or minimal TMPRSS2. In the endocytic pathway, the virus activation is driven by successful internalization, proteolysis and processing in endosomes/lysosomes, a process typically enhanced by an acidic endosomal pH [7]. Angiotensin-converting enzyme 2 (ACE2) has been reported as the cellular receptor for both SARS-CoV-1 and SARS-CoV-2 [8–10]. However, we still lack the detailed understanding of the cell endocytic process of how SARS-CoV-2 enters the host cells after binding to the ACE2 receptor.

* Corresponding authors at: National Joint Engineering Research Center of Biodiagnostics and Biotherapy, Second Affiliated Hospital, Xi'an Jiaotong University, 710004 Xi'an, China.
E-mail addresses: mengliesu@xjtu.edu.cn (L. Meng), lushemin@xjtu.edu.cn (S. Lu).
[1] Contribute equally.

Viruses typically make use of various endocytic mechanisms physiologically directed to promote the absorption of fluids, solutes, and small particles. Briefly, the endocytosis pathways could be divided into dynamin-dependent pathways such as clathrin-mediated endocytosis (CME), caveolin-mediated endocytosis (CaME), fast endophilin-mediated endocytosis (FEME), and dynamin-independent pathways including macropinocytosis and lipid rafts, all of which have been studied in the context of virus entry [3,11]. A number of viruses including vesicular stomatitis viruses (VSV), Influenza A and Semliki forest take advantage of CME pathway to enter host cells [12,13]. A number of adaptors, scission factors, cytoskeleton and regulatory factors participate in this process, such as dynamin 2, AP-2, Eps15, epsin1, actin, Rab5, Rab7, PI(3,4)P and PI(4,5)P2 [3,14]. CaME is another important pathway for viruses to enter host cells and caveolin1 is necessary (and perhaps sufficient) for caveolar biogenesis. Simian virus 40 (SV40) has been widely studied and proposed to enter cells by CaME [15–17]. Recently, it was reported that SV40 particles enter the cell by binding to the carbohydrate moiety of the GM1 ganglioside in the plasma membrane of the host cell [18]. CaME is dynamin 2-dependent and is closely related to actin, Rab5, tyrosine kinases, phosphatases and protein kinase C (PKC) [3,19]. In 2015, Boucrot et al. found a new endocytic route called FEME, which is mediated by endophilin and independent of clathrin and AP-2. FEME can be blocked by inhibitors of dynamin, Rac, phosphatidylinositol-3-OH kinase, PAK1 and actin polymerization, and be activated upon CDC42 inhibition [20]. Endophilin A2 has also been found to be associated with enterovirus 71 (EV71) entry [21], exocytosis of neurosecretory vesicles [22], and early uptake structures that are induced by the bacterial Shiga and cholera toxins [23].

Importantly, SARS-CoV entry into host cells has been shown to occur through a novel clathrin- and caveolin-independent endocytic pathway, suggesting an involvement of dynamin-independent pathways [7]. Macropinocytosis, also known as cell drinking, is characterized by the formation of large (greater than200 nm in diameter) and ruffled protrusions of the cell membrane, driven by actin rearrangements, which is primarily mediating non-selective internalization of fluid and membrane [24]. Vaccina virus mature virion (VV MV), adenovirus 3 (Ad3), coxsackievirus B (CVB), herpes simplex virus 1 (HSV1), echovirus 1 (EV1) and Zaire ebolavirus (ZEBOV) were found to be depended on macropinocytosis for its internalization and infection [24–28]. Macropinocytosis is characterized by the involvement of cell signaling factors PAK1, PI(3)K, PKC, Akt, PKC, PLCc, Rab34 and PLC-A2 that act to promote membrane ruffling by stimulating actin remodeling through CDC42 and Rac [24]. Lipid rafts are liquid-ordered membranes, enriched in cholesterol and sphingolipids, involved in biosynthetic transport, endocytosis and signal transduction. Viruses are also believed to take advantage of lipid rafts for entry into their cell host, assembly, and budding [29]. For several viruses, membrane rafts have been suggested to be involved in the mediation of the entry of enveloped viruses, including influenza virus, Sindbis virus (SIN), human immunodeficiency virus (HIV), murine leukemia virus (MLV), measles virus, Ebola virus and SARS-CoV [29–34]. In addition, other endocytic pathways such as IL-2, ADP-ribosylation factor 6 (Arf6) and flotillin-dependent pathways have also been studied regarding their importance for viral entry [3,35,36]. However, the exact pathway for the entry to the host cells of SARS-CoV-2 is still unclear.

As SARS-CoV-2 is highly contagious, studies on this virus must be handled in biosafety level 3 or 4 containment laboratories, which often hinders pathological research of the SARS-CoV-2 and development of vaccine. Pseudoviruses are deprived of critical gene sequences of importance for virulence, while envelopes of these viral particles could have similar conformational structures as wild-type viruses, making it feasible to be handled in biosafety level 2 laboratories [37]. Particularly, the artificially inserting reporter sequences of luciferase and green fluorescence protein (GFP) makes the pseudoviruses to be a powerful tool for studying early infection events in the life cycle of SARS-CoV-2. Here, we used SARS-CoV-2 spike-bearing pseudoviruses to infect HEK293T-ACE2^{hi} cells, and characterized the contribution of each endocytic pathway to the entry and infection of pseudoviruses by quantitative analysis of luminescence and fluorescence intensity. The cholesterol-rich lipid rafts and endosomal acidification dependence of SARS-CoV-2 infection was finally clarified. This study provides novel information regarding the entry of SARS-CoV-2, which is likely to be useful in understanding the pathological characteristics of this virus, and also provide attractive therapeutic targets to block SARS-CoV-2 infections.

2. Materials and methods

2.1. Cells and culture

In order to examine the infection of SARS-CoV-2 pseudoviruses, we obtained an HEK293T cell line which stably and highly expressed human ACE2. HEK293T cells were from ATCC and HEK293T-ACE2^{hi} cells were constructed by Genomeditech (Shanghai, China) [38]. Briefly, HEK293T-ACE2^{hi} cells were produced by constructing hACE2 overexpression vector (pGMLV-PA6) and using lentivirus (pGMLV-CMV-H-ACE2-PGK-Puro) to infect the target cells to construct a stable cell line. HEK293T cells were cultured in DMEM high glucose medium (Hyclone, USA) containing 10% FBS (HyClone, USA) and 1% penicillin–streptomycin at 37 °C in a humidified atmosphere of 5% CO_2. HEK293T-ACE2^{hi} cells were maintained in DMEM with 10% FBS, 1% penicillin–streptomycin and 4 μg/ml puromycin at 37 °C in a humidified atmosphere of 5% CO_2.

2.2. Inhibitors, antibodies, and reagents

Chloroquine, the purity of 98%, was from Macklin (Shanghai, China). Hydroxychloroquine, the purity of 98%, was provided by Energy Chemical, (Shanghai, China). Ammonium chloride (NH_4Cl) and bafilomycin A1 were purchased from Sigma-Aldrich (St. Louis, MO, USA). Chemical inhibitors used in the drug inhibition assays including dynasore (Cat. No. HY-15304), chlorpromazine hydrochloride (CPZ) (Cat. No. HY-B0407A), 5-(N-ethyl-N-isopropyl) amiloride (EIPA) (Cat. No. HY-101840), IPA-3 (Cat. No. HY-15663), NSC 23,766 trihydrochloride (Cat. No. HY-15723A), methyl-β-cyclodextrin (MβCD) (Cat. No. HY-101461), ML141 (Cat. No. HY-12755) were purchased from Med Chem Express (MCE, USA). Mouse anti-endophilin A2 monoclonal antibody (sc-365704) was purchased from Santa Cruz Biotechnology (CA, USA). Rabbit anti-Caveolin-1 polyclonal antibody (abs122936) was purchased from Absin Bioscience Inc (Shanghai, USA). Rabbit anti-GAPDH polyclonal antibody (bs-2188R) was purchased from BIOSS (Beijing, China). Lipo8000 Transfection Reagent was purchased from Beyotime Biotechnology (Shanghai China). Luciferase Assay System kit (Cat. No. E1500) was provided by Promega (USA). The SARS-CoV-2 spike-bearing pseudovirus were purchased from Sino Biological (Cat. No. PSV001) (Beijing, China) and Biodragon (Cat. No. BDAA0026) (Beijing, China). The pseudoviruses were produced in HEK293T cells with a retrovirus backbone, which membrane surface contains the S protein of SARS-CoV-2, and the RNA sequence of green fluorescent protein (zsGreen) and luciferase is packaged in its genome.

2.3. Cytotoxicity assay

Cell viability was evaluated using a cell counting kit 8 (CCK-8) (Bimake, USA) and following the manufacturer's instructions. Briefly, HEK293T-ACE2^{hi} cells were seeded into 96-well plates at a density of five thousand cells per well and then treated with different concentrations of chemical inhibitors for 24 h, and then 10 μl of CCK-8 solution was added to each well followed by an additional 2 h incubation at 37 °C. Relative cell viability was assessed by monitoring the absorption at 450 nm using a multiskan spectrum (Thermo, USA). The percentage of viable cells was calculated using the formula: $[(OD_{Treated} - OD_{Blank}) / (OD_{Control} - OD_{Blank})] \times 100\%$. Each sample was assayed with four replicates per measurement, and each experiment was repeated three times.

2.4. Pseudovirus infection assay

The SARS-CoV-2 spike-bearing pseudovirus infection assays were conducted as described previously [38]. In brief, 2×10^4 of HEK293T-ACE2^{hi} cells were seeded into white 96-well plates. SARS-CoV-2 spike-bearing pseudoviruses (multiplicity of infection (MOI) = 10) were added into medium and incubated in a 37 °C incubator containing 5% CO_2 for 4 h. Subsequently, cells were washed once with PBS and replaced by 200 μl of fresh DMEM. To test the pseudovirus infection, the luciferase luminescence was detected by a microplate reader (Thermo Electron Corporation) and the GFP in HEK293T-ACE2^{hi} cells was observed with a fluorescence microscope (Nikon, Japan).

2.5. siRNA assay

siRNA against endophilin A2 (si-EA2) (5′-GCU GGA UGA UGA CUU CAA A-3′, 5′-UUU GAA GUC AUC AUC CAG C-3′) clathrin (si-clathrin) (5′-GAG GUC AAU UCU CUA CUG A-3′, 5′-UCA GUA GAG AAU UGA CCU C-3′), dynamin (si-dynamin) (5′-CCG CAG CCA GAA GGA UAU U-3′, 5′-UUU GAA GUC AUC AUC CAG C-3′) and caveolin-1 (si-CAV1) (5′-CCA GAA GGG ACA CAC AGU U-3′, 5′-AA CUGUGUGUCCCUUCUGG-3′) were designed and produced by GenePharma (Shanghai, China), and nonspecific siRNA sequences were used as a control (si-NC). The siRNA was transfected into HEK293T-ACE2^{hi} cells using Lipo8000 Transfection Reagent according to the manufacturer's instructions. The protein levels of EA2 and caveolin 1 were tested by Western blotting to evaluate the silence efficiency before the subsequent assays were performed. For the infection assay, HEK293T-ACE2^{hi} cells transfected with siRNA were incubated with SARS-CoV-2 spike-bearing pseudoviruses for 4 h, and then the unbound pseudovirus were removed by washing with PBS, and cells were incubated in fresh DMEM medium. The GFP fluorescence intensity and luciferase activity were detected at indicated time points.

2.6. Virus infection in the presence of inhibitors

HEK293T-ACE2^{hi} cells were pre-treated with different concentrations of inhibitors (chloroquine, hydroxychloroquine, NH_4Cl, bafilomycin A1, dynasore, CPZ, EIPA, NSC 23,766 trihydrochloride, IPA-3, MβCD or ML141) for 1 h and then incubated with SARS-CoV-2 spike-bearing pseudoviruses at 37 °C in a humidified atmosphere of 5% CO_2 for 4 h. In these total 5 h, the inhibitors were present in the medium. Subsequently, the unbound pseudoviruses were removed by washing with PBS, and cells were incubated in fresh DMEM medium. At different time points, the GFP fluorescence intensity and luciferase activity were detected.

2.7. Cholesterol supplement

For cholesterol supplement experiments, cells, firstly pre-treated with MβCD (2.5 mM) for 1 h, were added with different concentration of cholesterol for 1 h, followed by the incubation of SARS-CoV-2 spike-bearing pseudoviruses (MOI = 10) for 4 h. In addition, cells were directly treated with different concentration of cholesterol for 1 h and incubated with SARS-CoV-2 spike-bearing pseudoviruses (MOI = 10) for 4 h.

2.8. Protein extraction and Western blotting

Total protein lysates from cells were extracted by using the RIPA solution (Beyotime, China) with a cocktail of protease and phosphatase inhibitors (Roche), followed with incubation on ice for 30 min and centrifugation at $12,000 \times g$ for 15 min at 4 °C. The final protein concentration of each sample was determined by a BCA kit (Thermo Scientific).

The protein expression level was detected by Western blotting analysis. The supernatants (20 μg total protein) from protein lysates were subjected to SDS-PAGE gel according to standard procedures in Bio-Rad system. Mouse anti-endophilin A2 antibody, rabbit anti-Caveolin-1and rabbit anti-GAPDH were used as the primary antibody. The signal was further detected by using the secondary antibody of goat anti-rabbit IgG or goat anti-mouse IgG. The intensity of specific binding bands was calculated against the endogenous control (GAPDH), and data were showed as fold change against the control.

2.9. Statistical analysis

Quantitative data were expressed as mean ± SEM. The statistical analysis of differences between experimental groups was performed using One-way ANOVA or Student's t-test. P value < 0.05 was considered significant.

3. Results

3.1. High expression of human ACE2 facilitates the infection of SARS-CoV-2 spike-bearing pseudoviruses

In this study, SARS-CoV-2 spike-bearing pseudoviruses were used to investigate the virus infection. They contain the sequences of GFP and luciferase (Fig. 1A), so that successful infection can be easily quantified by detecting the fluorescence intensity of GFP or luminescent intensity of luciferase, even with minute amounts of pseudoviruses. It has been shown that SARS-CoV-2 uses its spike protein binding ACE2 receptors to invade host cells [39]. We used SARS-CoV-2 pseudoviruses to infect HEK293T cells and HEK293T-ACE2^{hi} cells. The luminescence intensity showing the luciferase activity was detected after 48 h incubation. It was found that the SARS-CoV-2 pseudoviruses only infected HEK293T-ACE2^{hi} cells and rarely entered to HEK293T cells (Fig. 1B and C). After incubation with pseudoviruses for 60 min, GFP expression could be observed in HEK293T-ACE2^{hi} cells and fluorescence intensity gradually increases with time. GFP expression was observed in the whole cell at 12 h post-infection with the pseudoviruses (Fig. 1D). The percentage of infected cells (with GFP expression) were also analyzed, and the result showed that it increased from 63% in 60 min to 91% in 12 h (Fig. 1D).

3.2. SARS-CoV-2 spike-bearing pseudoviruses are internalized through endocytosis sensitive to pH

The established view on the endocytic pathway of viruses is that it is pH-dependent and involve an activation step of the endocytosed
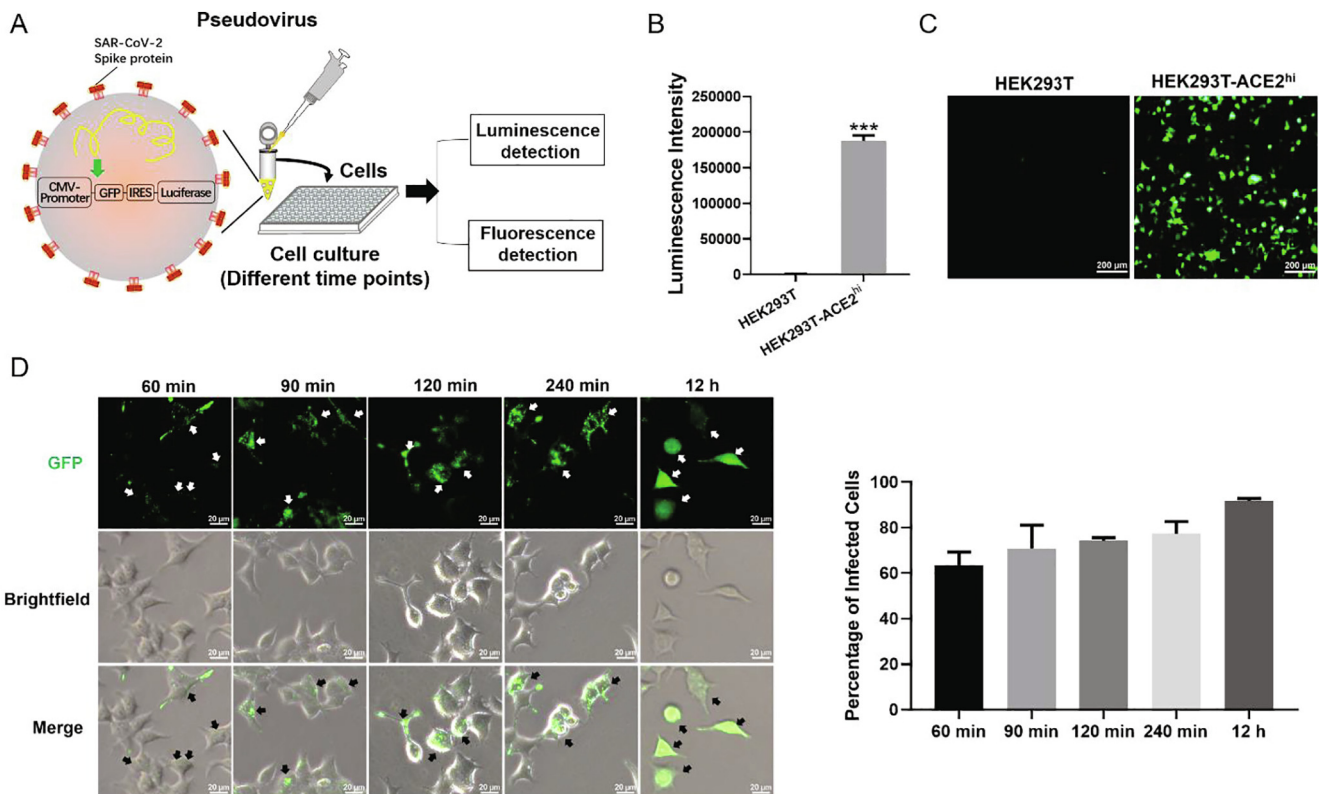
Fig. 1. SARS-CoV-2 spike-bearing pseudovirus entering cells is ACE2-dependent. (A) Schematic of SARS-CoV-2 spike-bearing pseudovirus infection and detection. GFP: green fluorescent protein; IRES: internal ribosome entry site. (B) HEK293T (n = 3) and HEK293T-ACE2hi cells (n = 3) were infected with SARS-CoV-2 spike-bearing pseudoviruses at MOI of 10. The unbound pseudoviruses were washed out at 4 h post-infection and the chemiluminescence was detected by a microplate reader at 48 h post-infection. (C) Fluorescence images are shown of HEK293T and HEK293T-ACE2hi cells at 48 h post-infection (MOI = 10). Scale bar indicates 200 μm. (D) HEK293T-ACE2hi cells were continuously infected with SARS-CoV-2 spike-bearing pseudovirus (MOI = 10) for 1 h, 1.5 h, 2 h, 4 h and 12 h, and live cells were visualized by fluorescent microscopy to locate the GFP protein. Scale bar indicates 20 μm. Statistical data is presented as the mean ± SD of three independent experiments with repeated three times. *** P < 0.001. (For interpretation of the references to colour in this figure legend, the reader is referred to the web version of this article.)

virions in the acidic endosome. The SARS-CoV enter cells via endocytosis based on observations using ACE2-GFP and chemical inhibitors for endosomal acidification [7]. To analyze the pathway of SARS-CoV-2 spike-bearing pseudovirus infection, lysosomotropic weak bases (such as chloroquine, hydroxychloroquine and ammonium chloride (NH_4Cl)) and a v-ATPase inhibitor (bafilomycin A1) were used to confirm that the viruses require low pH for infection [3]. All inhibitors used were tested on HEK293T-ACE2hi cells by cytotoxicity assays to obtain the proper working concentration range (Fig. S1A-D). As shown in Fig. 2A-D, pretreatment with different concentrations of inhibitors for endosomal acidification all significantly decreased viral infectivity in a dose-dependent manner. After incubation of HEK293T-ACE2hi cells with pseudoviruses for 48 h, chloroquine (20 μM), hydroxychloroquine (20 μM), NH_4Cl (50 mM) and bafilomycin A1 (100 nM) respectively caused 77% (Fig. 2A), 73% (Fig. 2B), 78% (Fig. 2C) and 99% (Fig. 2D) reduction in pseudovirus infection by detecting the luciferase luminescence value. We found that green fluorescence was seen in whole cells infected with SARS-CoV-2 spike-bearing pseudoviruses, while the green fluorescence intensity in cells pretreated with different endosomal acidification inhibitors was significantly reduced at 12 h post-infection with the pseudoviruses (Fig. 2E). These results demonstrate that the infection of SARS-CoV-2 spike-bearing pseudoviruses is via endocytosis and pH-dependent.

3.3. Dynamin related endocytic pathways are not involved in SARS-CoV-2 spike-bearing pseudovirus infection

CME, CaME, as well as FEME, are the most studied pathways to be involved in virus internalization [3,20]. To identify the specific

endocytic pathway of SARS-CoV-2, siRNA and biochemical inhibitors targeting each endocytic pathway were used to evaluate the effect on SARS-CoV-2 spike-bearing pseudovirus infection. Our results indicated that the clathrin-, caveolar-, and endophilin A2-dependent pathway are not likely to be involved in the SARS-CoV-2 spike-bearing pseudovirus infection. Chlorpromazine (CPZ) is a drug commonly used to inhibit clathrin-mediated endocytosis and prevent the assembly of clathrin coating pits on the cell surface [40,41]. We obtained the proper working concentration range of CPZ by cytotoxicity assays (Fig. S1E). Our result showed that CPZ pretreatment did not affect the luciferase and fluorescence signal compared with vehicle control treated cells at 24 h and 48 h post-infection with the SARS-CoV-2 spike-bearing pseudoviruses, while infection of VSV-G pseudoviruses as a positive control was inhibited by CPZ pretreatment (Fig. 3A and B, Fig. S2A). We also used RNAi method to explore the role of clathrin in SARS-CoV-2 spike-bearing pseudovirus infection. Silencing of clathrin showed similar results in luciferase luminescence, compared with the results using clathrin inhibitors (Fig. 3C). Next we used a siRNA approach to explore the role of CaME in SARS-CoV-2 spike-bearing pseudovirus infection. The silencing efficiency of cavelin-1 (CAV1) siRNA in HEK293T-ACE2hi cells was detected by Western blotting (Fig. 3D). Silencing of CAV1 failed to show any significant effect on infection of spike-bearing pseudoviruses by monitoring the luminescence intensity of luciferase (Fig. 3D). We next investigated whether FEME was related to SARS-CoV-2 spike-bearing pseudovirus infection by knocking down EA2 using its specific siRNA, and the silencing efficiency of EA2 siRNA was also detected by Western blotting (Fig. 3E). In line with silencing of CAV1, silencing of EA2 displayed no effect on spike-bearing pseudovirus infec-
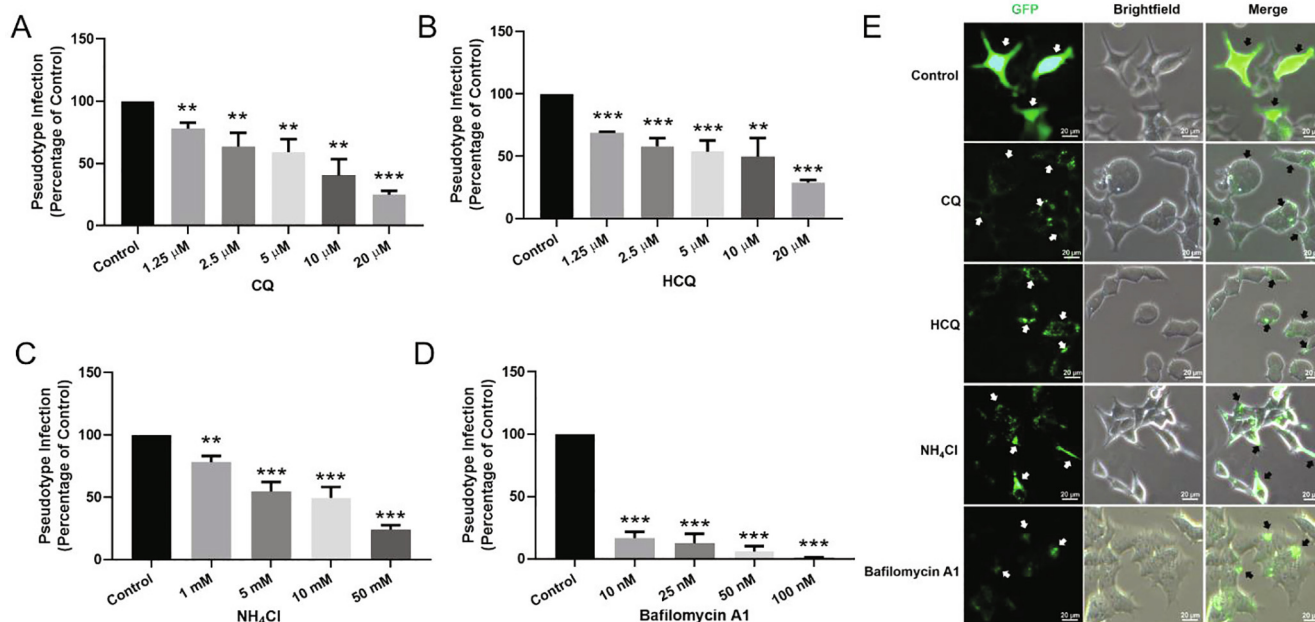
Fig. 2. Inhibition of endosomal acidification prevents SARS-CoV-2 spike-bearing pseudovirus infection. (A–D) HEK293T-ACE2^{hi} cells were pre-treated with different doses of chloroquine (n = 3) (A), hydroxychloroquine (n = 3) (B), NH$_4$Cl (n = 3) (C) and bafilomycin A1 (n = 3) (D) then infected with SARS-CoV-2 spike-bearing pseudoviruses at MOI of 10. The pseudoviruses infectivity was analyzed by luciferase activity at 48 h post-infection. (E) Fluorescence pictures and brightfield are shown of control, chloroquine (20 μM), hydroxychloroquine (20 μM), NH$_4$Cl (50 mM) and bafilomycin A1 (100 nM) at 12 h post-infection. Scale bar indicates 20 μm. Statistical data is presented as the mean ± SD of three independent experiments with repeated three times. [**] P < 0.01, [***] P < 0.001.

tion in HEK293T-ACE2^{hi} cells compared to the siNC control (Fig. 3E). This result probably suggested that EA2 might not contribute to the pseudovirus infection, however, we remain not to completely rule out the FEME pathway due to the compensation effect from the other endophilin isoforms.

Dynamin is a cellular GTPase and plays an essential role in some modes of endocytosis, including CME, FEME, CaME as well as some of the non-clathrin/non-caveolin-dependent pathways [42]. Accordingly, viruses may use either dynamin-dependent or - independent modes of endocytosis or a combination of the two [43]. Our above results indicated that dynamin-related pathways are not likely to be involved in the entry of SARS-CoV-2. To double confirm our finding we used dynasore, an effective endocytic pathway inhibitor that could inhibit dynamin activity by rapidly blocking coated vesicle formation within seconds of dynasore addition [42]. The proper working concentration range of dynasore was obtained by cytotoxicity assays in HEK293T-ACE2^{hi} cells (Fig. S1F). Results showed that pretreatment of dynasore at different concentrations did not affect SARS-CoV-2 spike-bearing pseudovirus infectivity by detection of luciferase luminescence at 48 h post-infection with the pseudoviruses (Fig. 3F and Fig. S2B), while infection of VSV-G pseudoviruses as a positive control was inhibited by dynasore pretreatment. The representative fluorescence image also showed that dynasore had no significant effect on SARS-CoV-2 spike-bearing pseudovirus infection (Fig. 3G). Knocking down of dynamin using siRNA showed similar results in luciferase luminescence compared with the results using dynasore (Fig. 3H).

3.4. SARS-CoV-2 spike-bearing pseudoviruses are internalized without involvement of macropinocytosis

Then we further investigated the dynamin-independent pathways in virus infection. Macropinosome formation requires a variety of cellular factors activity, such as Na$^+$/H$^+$ exchange (NHE), PKC, p21-activated kinase 1 (PAK1) and Rho GTPase (CDC42 and RAC1)

[24,44,45]. We assessed the role of macropinocytosis in SARS-CoV-2 spike-bearing pseudovirus infection using 5-(N-ethyl-N-isopropyl) amiloride (EIPA, an inhibitor of NHE) [46], NSC 23,766 trihydrochloride (an inhibitor of RAC1) [47], IPA-3 (an inhibitor of PAK1) [48]. All inhibitors used were tested on HEK293T-ACE2^{hi} cells by cytotoxicity assays to obtain the proper working concentration range (Fig. S1G-I). As shown in Fig. 4A, EIPA pretreatment decreased SARS-CoV-2 spike-bearing pseudovirus infectivity, only when the concentration of EIPA reaches 80 μM. IPA-3 pretreatment exhibited no statistically significant change on the percentage of pseudovirus infection efficiency (Fig. 4B). A dose-dependent increase of SARS-CoV-2 spike-bearing pseudovirus infection was observed in the presence of NSC 23,766 trihydrochloride (Fig. 4C). The result of GFP observed under a fluorescence microscope to evaluate pseudovirus infection is similar to the result of luciferase luminescence (Fig. 4D). In summary, these results indicate that macropinocytosis is likely not involved in the mediation of the infection of SARS-CoV-2 spike-bearing pseudoviruses.

3.5. SARS-CoV-2 spike-bearing pseudoviruses invades host cells in dependence on cholesterol-rich lipid rafts

Cholesterol-rich lipid rafts have been found to play a crucial role in the interaction between the SARS-CoV S protein and ACE2 [34,49]. To investigate the involvement of cholesterol-rich lipid rafts during the initial steps of SARS-CoV-2 infection, we used methyl-β-cyclodextrin (MβCD) to deplete cholesterol from HEK293T-ACE2^{hi} cells. The proper working concentration range of MβCD was obtained by cytotoxicity assays in HEK293T-ACE2^{hi} cells (Fig. S1J). MβCD, which captured cholesterol and thereby sequestered cholesterol from the plasma membrane, was able to block SARS-CoV-2 spike-bearing pseudovirus infection in a dose-dependent manner (Fig. 5A and B). When the concentration of MβCD pretreatment reached 2.5 mM, the inhibition efficiency exceeded 96% compared to vehicle control treatment cells at 48 h post-infection with the SARS-CoV-2 spike-bearing pseu-
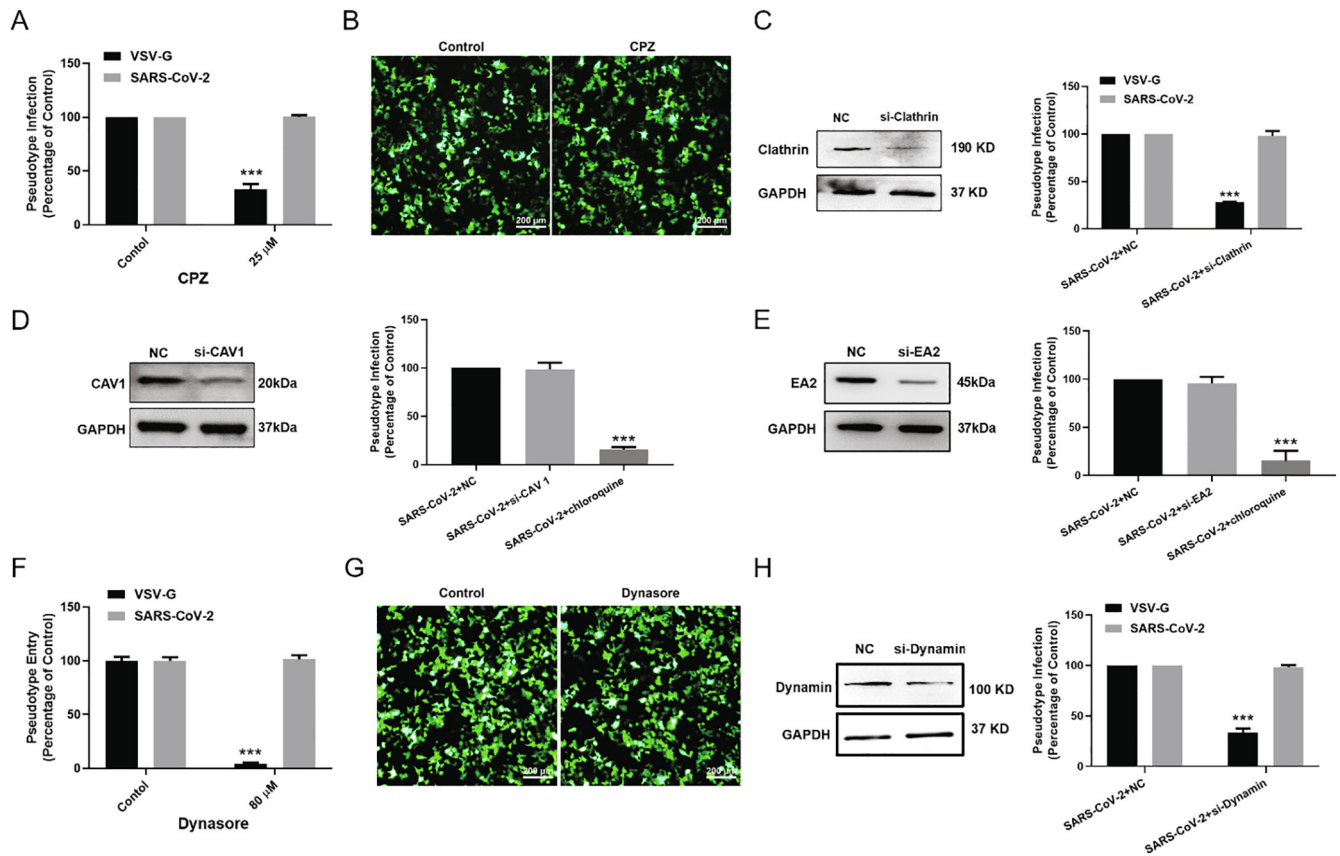
Fig. 3. SARS-CoV-2 spike-bearing pseudovirus infection of HEK293T-ACE2hi cells is independent of dynamin, clathrin, caveolin, and endophilin A2. (A) HEK293T-ACE2hi cells were pre-treated with CPZ (25 μM) (n = 3) and infected with SARS-CoV-2 spike-bearing pseudoviruses (MOI = 10) or the control pseudoviruses VSV-G (n = 3). The infection was then measured by firefly luciferase activity at 48 h post-infection. (B) Fluorescence images of cells are shown of control and pretreatment with CPZ (25 μM) at 48 h post-infection with SARS-CoV-2 spike-bearing pseudoviruses (MOI = 10). Scale bar indicates 200 μm. (C-E) HEK293T-ACE2hi cells were transfected with si-Clathrin (C) si-CAV1 (D) or si-EA2 (E) and then infected with SARS-CoV-2 spike-bearing pseudoviruses (MOI = 10), and infectivity of with si-Clathrin (n = 3) (C) si-CAV1 (n = 3) (D) or si-EA2 (n = 3) (E) was measured by firefly luciferase activity at 48 h post-infection. (G, H) HEK293T-ACE2hi cells were pre-treated with dynasore (80 μM) (n = 3), and infected with SARS-CoV-2 spike-bearing pseudoviruses (MOI = 10) or the control pseudoviruses VSV-G (n = 3). The infection efficiency was evaluated as above mentioned. (H) HEK293T-ACE2hi cells were transfected with si-Dynamin and then infected with SARS-CoV-2 spike-bearing pseudoviruses (MOI = 10) or VSV-G pseudoviruses (MOI = 10), and infectivity was measured by firefly luciferase activity at 48 h post-infection (n = 3). Scale bar indicates 200 μm. Statistical data is presented as the mean ± SD of three independent experiments with repeated three times. *** P < 0.001.

doviruses. As negative control, the infection of VSV-G pseudoviruses was not affected by cholesterol depletion (Fig. 5A). HEK293T-ACE2hi cells were treated with 2.5 mM MβCD at different time points and inoculated with SARS-CoV-2 spike-bearing pseudoviruses for viral infection. As shown in Fig. 5C, when MβCD was pre-treated to cells (pre-2 h, pre-1 h, pre-0.5 h, 0 h), pseudovirus infection was significantly reduced by MβCD pretreatment; whereas MβCD treatment at 1 h post infection had no effect on viral infection. This indicated that cholesterol mainly affected the process before the virus entered the cells. The infection and infection of SARS-CoV-2 spike-bearing pseudoviruses could be restored by supplement of exogenous cholesterol. MβCD-treated HEK293T-ACE2hi cells with exogenous cholesterol (100 μg/ml) showed almost twice the total number of luciferase luminescence compared to cells treated with pseudoviruses only. (Fig. 5D and E). In addition, we also tested the effect of supplementing exogenous cholesterol on pseudovirus infection, and found that different concentrations of cholesterol all increased pseudovirus infection (Fig. 5F). Hence, it demonstrates that the anti-SARS-CoV-2 spike-bearing pseudovirus infection of MβCD is dependent on cholesterol depletion. The clathrin-independent carriers (CLIC) and GPI-anchored-protein-enriched endosomal compartments (GEEC) pathway is an important endocytic pathway for cholesterol-rich lipid raft components [14,50]. The CLIC/GEEC

pathway has been demonstrated to be regulated by GRAF1, CDC42 and Arf1 [51–53]. We tried to preliminarily assess the role of CLIC/GEEC pathway in SARS-CoV-2 spike-bearing pseudovirus infection using MLL141 (an inhibitor of CDC42) [54,55]. The MLL141 was tested on HEK293T-ACE2hi cells by cytotoxicity assays to obtain the proper working concentration range (Fig. S1K). The result showed that MLL141 (10 μM) pretreatment exhibited no statistically significant change on the pseudovirus infection (Fig. 5G), suggesting that CDC42-involved CLIC/GEEC pathway probably might not participate in the infection of SARS-CoV-2.

4. Discussion

The SARS-CoV-2 virus infection initiated with binding of viral particles to host surface ACE2 receptors, is a crucial step for effective viral infection. Using SARS-CoV-2 pseudoviruses we could show that cholesterol-rich membrane lipid raft plays a major role in the infection and not the classical endocytosis pathways, such as clathrin-, caveolin-, endophilinA2-mediated endocytosis and macropinocytosis.

SARS-CoV-2 is a positive-stranded RNA virus belonging to the β coronavirus genus. The structure of this new coronavirus is mainly composed of single-stranded RNA, membrane (M), nucleocapsid
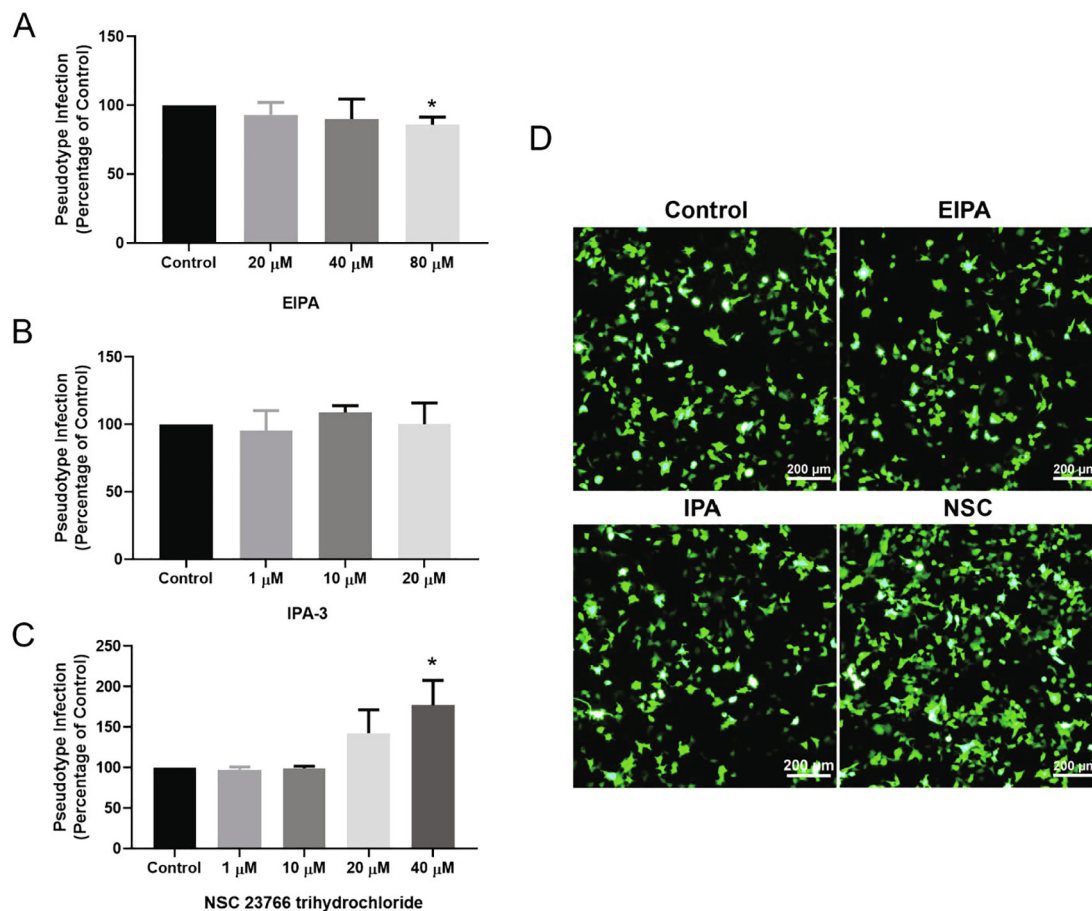
Fig. 4. SARS-CoV-2 spike-bearing pseudoviruses infects cells independent with macropinocytosis. (A–C) HEK293T-ACE2^{hi} cells were pre-treated with different concentrations of EIPA (n = 3) (A), IPA-3 (n = 3) (B), and NSC 23,766 trihydrochloride (n = 3) (C), and then infected with SARS-CoV-2 spike-bearing pseudoviruses at MOI of 10. The pseudoviruses infectivity was analyzed by firefly luciferase activity at 48 h post-infection. (D) Fluorescence images are shown of control, EIPA (80 μM), IPA-3 (20 μM), and NSC 23,766 trihydrochloride (40 μM) at 24 h post-infection with SARS-CoV-2 spike-bearing pseudoviruses. Scale bar indicates 200 μm. Statistical data is presented as the mean ± SD of three independent experiments with repeated three times. * P < 0.05.

(N), envelope (E), and S proteins [56]. The N protein, one of the most abundant viral proteins, combines with viral genomic RNA to form a ribonucleoprotein (RNP) complex [57]. It showed that N protein mainly involved in viral mRNA transcription and replication and cytoskeletal and immune regulation of host cells [58]. The M protein of SARS-CoV-2 can inhibit IFN-β promoter activation and participate in evading host anti-viral immunity [59]. E protein relates to the virus pathogenicity and may activate the host's inflammatory response. In some coronaviruses, the E protein deletion will reduce the virus's toxicity [60]. S protein directly binds to the host cell membrane receptor to mediate SARS-CoV-2 entry [61]. Pseudoviruses are useful virological tools because of their safety and versatility, and the pseudovirus expressing S-protein has been shown to be used to study the mechanism of SARS-CoV-2 entry [5,62,63] and neutralization assays [64].

TMPRSS2 have been shown to cleave SARS-CoV-2 S protein and enhance membrane fusion [6,65]. The camostat mesylate (an inhibitor of TMPRSS2) can partially block SARS-CoV-2 infection of the Caco-2 cells (TMPRSS2^{+}), while it did not interfere with SARS-CoV-2 infection of the Vero and HEK293T cells (TMPRSS2^{−}) [5,65,66]. In contrast, the entry of SARS-CoV-2 mainly depends on the endosomal pathway in Vero and HEK293T cells that do not express TMPRSS2, and can be inhibited by E-64d (cathepsins B/L inhibitor) [5,66]. Consistent with these findings, Zhu *et al* [6] showed that SARS-CoV-2 entered cells via two pathways. One pathway was the membrane fusion pathway that relied on pro-

teases (e.g., TMPRSS2), and the other pathway was the endosomal pathway, which is less efficient than the plasma membrane fusion pathway. In the present study, we focused on the cell endosomal pathways, which remained poorly understood by now, using the SARS-CoV-2 spike-bearing pseudoviruses and HEK293T cell line (TMPRSS2^{−}) as research tools.

Previous studies have shown that SARS-CoV S protein and its interaction with the cell receptor ACE2 is essential for SARS-CoV entry and membrane fusion [67,68]. Recent studies also highlighted the important role of ACE2 in mediating the SARS-CoV-2 entry [69,70]. Compared with SARS-CoV, the ACE2 receptor binding domain of SARS-CoV-2 differs on several key amino acid residues which leads to a stronger binding affinity with receptor and may account for the greater pathogenicity of SARS-CoV-2 [56,71]. In this study, we also confirmed the important role of ACE2 in SARS-CoV-2 infection.

The chloroquine and hydroxychloroquine have been demonstrated to inhibit SARS-CoV-2 effectively *in vitro* [38,72]. Howerve, some subsequent studies have found that chloroquine targets the viral activation which is not actived in lung cells and is unlikely to prevent the infection of SARS-CoV-2 in related patients, while the use of chloroquine was associated with an increased risk of denovo ventricular arrhythmia during hospitalisation [73,74]. We found that NH₄Cl and bafilomycin A1 also had inhibitory effect to SARS-CoV-2 pseudovirus infection as chloroquine, and bafilomycin A1 had a better inhibitory effect than chloroquine in HEK293T-
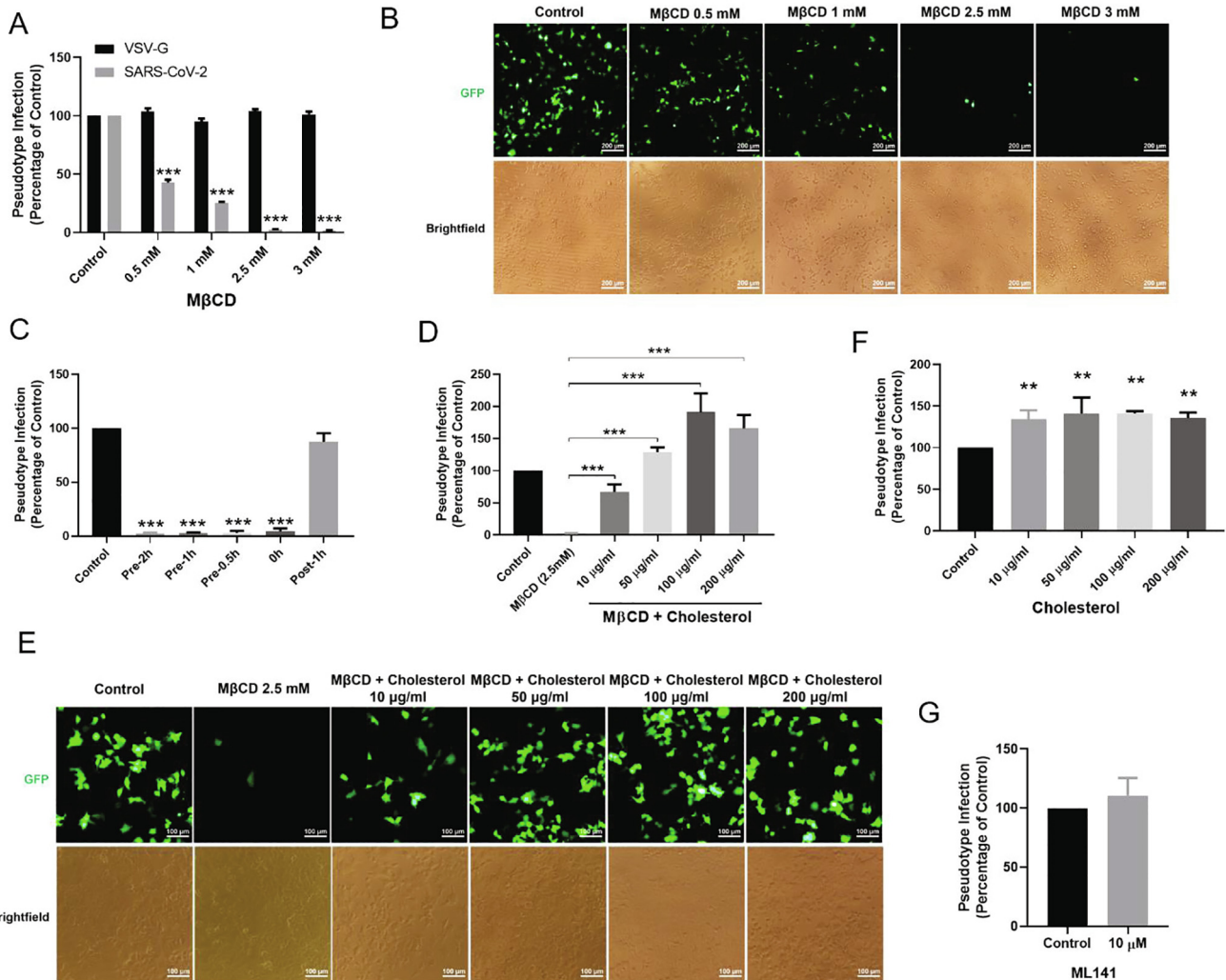
Fig. 5. The infection of SARS-CoV-2 spike-bearing pseudoviruses is cholesterol dependent. (A) HEK293T-ACE2^{hi} cells were pre-treated with MβCD at different concentrations (n = 3), and then infected with SARS-CoV-2 spike-bearing pseudoviruses (MOI = 10) or the control pseudoviruses VSV-G (n = 3). The infection was measured by firefly luciferase activity at 48 h post-infection. (B) Fluorescence and brightfield images are shown of control and pretreatment with different concentrations of MβCD at 4 h post-infection. Scale bar indicates 200 μm. (C) Time frame of MβCD treatment. HEK293T-ACE2^{hi} cells were treated with 2.5 mM MβCD at indicated time points and infected with SARS-CoV-2 spike-bearing pseudoviruses at MOI of 10. The infectivity was analyzed by firefly luciferase activity at 48 h post-infection. (D) HEK293T-ACE2^{hi} cells were pre-treated with MβCD for 1 h, and then different concentrations of supplement of exogenous cholesterol were added for 1 h, followed by the incubation of SARS-CoV-2 spike-bearing pseudoviruses (MOI = 10) for 4 h. The infectivity was analyzed by firefly luciferase activity at 48 h post-infection. (E) Fluorescence and brightfield images are shown of control, pretreatment with MβCD and MβCD + cholesterol at 48 h post-infection with pseudoviruses. Scale bar indicates 200 μm. (F) HEK293T-ACE2^{hi} cells were pre-treated with cholesterol at different concentrations (n = 4) and then infected with SARS-CoV-2 spike-bearing pseudoviruses (MOI = 10). (G) HEK293T-ACE2^{hi} cells were pre-treated with ML141 (10 μM) (n = 3) for 1 h and infected with SARS-CoV-2 spike-bearing pseudoviruses (MOI = 10) for 4 h. The infection was then measured by firefly luciferase activity at 24 h post-infection. Statistical data is presented as the mean ± SD of three independent experiments with repeated three times. [**] P < 0.01, [***] P < 0.001.

ACE2^{hi} cells. Our data provide additional information that inhibition of endosome acidification can be used for anti-SARS-CoV-2 infections drug design.

Lipid rafts represent foci for mediating signal transduction and protein trafficking and increasing evidence shows that lipid rafts are essential in the replication cycle of different viruses [29,75]. Biochemical fractionation and confocal imaging confirmed that ACE2 colocalized with lipid raft marker ganglioside monosialotetrahexosylganglioside1 (GM1) and upon cholesterol depletion by MβCD treatment inhibited infectivity of SARS-CoV pseudoviruses by 90% [34]. Cholesterol depletion with MβCD inhibited the infectivity and the receptor binding ability of Newcastle disease virus (NDV) [76]. Cholesterol-rich lipid rafts are required for release of infectious human respiratory syncytial virus (RSV) [77]. Strong data also suggest that virus budding can occur within membrane lipid rafts [3,29,31]. It has been reported that

the budding of HIV virions through lipid rafts whereby host cell cholesterol, sphingolipids, and GPI-linked proteins within these domains are incorporated into the viral envelope [78]. Host lipid rafts play a critical role in binding, endocytosis, assembly and budding of influenza A virus (IAV) [79].

Therefore, a role for cholesterol has attracted increasing attention for the understanding of the SARS-CoV-2 infection process [62,80,81]. It has been reported that cholesterol 25-hydroxylase (CH25H) inhibits SARS-CoV-2 and other coronaviruses by depleting membrane cholesterol *in vitro* and in COVID-19-infected patients [62]. Observational studies on COVID-19 individuals with underlying cardiovascular disease (CVD) showed that they increased the severity of the disease and mortality [82]. The Chinese Center for Disease Control and Prevention published the case series to date of COVID-19 in mainland China (72,314 cases, updated through February 11, 2020), with an overall case-fatality
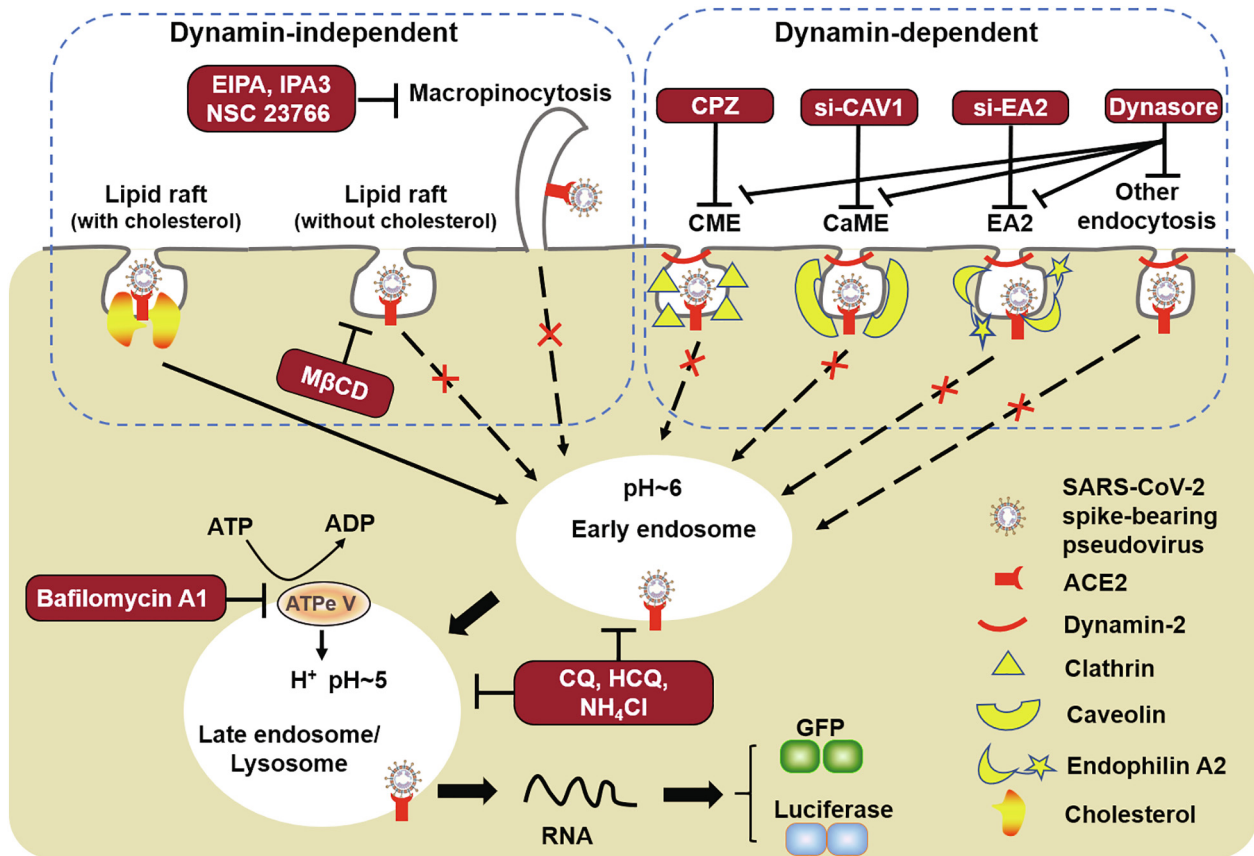
Fig. 6. Graphical summary of SARS-CoV-2 spike-bearing pseudovirus infection.

rate (CFR) was 2.3%. Importantly, the CFR with underlying CVD patients was the highest among those with preexisting comorbid conditions, increased to 10.5% (7.3% for diabetes, 6.3% for chronic respiratory disease, 6.0% for hypertension, and 5.6% for cancer) [83]. Statins are lipid-lowering therapeutics with favorable anti-inflammatory profiles and have been proposed as an adjunct therapy for COVID-19 [84,85]. The retrospective study on 13,981 patients with COVID-19 in Hubei Province, China, among which 1,219 received statins showed that the risk for 28-day all-cause mortality was 5.2% and 9.4% in the matched statin and non-statin groups respectively [84]. Combined with the results of this study, statins may inhibit SARS-CoV-2 infections by lowering cholesterol. In this study, we proved that SARS-CoV-2 spike-bearing pseudovirus infection are associated with cholesterol-rich lipid rafts. Meanwhile, we preliminarily studied the CLIC/GEEC pathway, which is an important lipid raft-related endocytic pathway. Adeno-associated virus 2 (AAV2) infection had been shown to require endocytosis through the CLIC/GEEC pathway [86]. The infection of AAV2 is dependent on membrane cholesterol and can be blocked by inhibition of the three main effectors of CLIC/GEEC pathway, GRAF1, CDC42 and Arf1 [86]. However, our result showed that inhibition of CDC42 had no effect on SARS-CoV-2 spike-bearing pseudovirus infection. Therefore, it remains not clear how cholesterol-rich lipid raft regulates SARS-CoV-2 binding or entry, which need to be studied further.

In conclusion, the present study provides evidence that the infection of SARS-CoV-2 spike-bearing pseudoviruses to HEK293T-ACE2^{hi} cells is via ACE2 receptor-dependent, pH-sensitive endocytosis and can be blocked by inhibitors for endosomal acidification. Moreover, classical endocytosis pathways, such as clathrin-, caveolin-, endophilinA2-mediated endocytosis and macropinocytosis are not involved in SARS-CoV-2 spike-bearing pseudovirus infection. Instead, cholesterol-rich membrane lipid raft may play a major role in the infection of SARS-CoV-2 spike-bearing pseudoviruses to HEK293T-ACE2^{hi} cells (Fig. 6).

Declaration of Competing Interest

The authors declare that they have no known competing financial interests or personal relationships that could have appeared to influence the work reported in this paper.

Acknowledgements

Data and materials availability: All data needed to evaluate the conclusions in the paper are present in the paper and/or the Supplementary Materials. Additional data related to this paper may be requested from the authors.

Author contributions: All authors contributed to the discussion, writing, and revising of the manuscript. X. L. and W.Z. designed the research, performed the experiments, including acquiring data and analyzing data, and wrote the manuscript. M. F. performed siRNA assay. J. Z. helped with cytotoxicity assay, ana-

lyzed the data, and revised the manuscript. Y. P. and F. H. performed some pseudovirus infection assays and analyzed the data. R.H. designed the research and revised the manuscript. L.M. and S.L. designed the research, analyzed the data, revised the manuscript, supervised and took the overall responsibility of the study.

Appendix A. Supplementary data

Supplementary data to this article can be found online at https://doi.org/10.1016/j.csbj.2021.04.001.

References

[1] Zhou P, Yang XL, Wang XG, et al. A pneumonia outbreak associated with a new coronavirus of probable bat origin. Nature 2020;579:270–3. https://doi.org/10.1038/s41586-020-2012-7.

[2] Shrock E, Fujimura E, Kula T, et al. Viral epitope profiling of COVID-19 patients reveals cross-reactivity and correlates of severity. Science 2020. https://doi.org/10.1126/science.abd4250.

[3] Mercer J, Schelhaas M, Helenius A. Virus entry by endocytosis. Annu Rev Biochem 2010;79:803–33. https://doi.org/10.1146/annurev-biochem-060208-104626.

[4] Smith AE, Helenius A. How viruses enter animal cells. Science 2004;304:237–42. https://doi.org/10.1126/science.1094823.

[5] Hoffmann M, Kleine-Weber H, Schroeder S, et al. SARS-CoV-2 cell entry depends on ACE2 and TMPRSS2 and is blocked by a clinically proven protease inhibitor. Cell 181 2020:271–280 e278. https://doi.org/10.1016/j.cell.2020.02.052.

[6] Zhu Y, Feng F, Hu G, et al. A genome-wide CRISPR screen identifies host factors that regulate SARS-CoV-2 entry. Nat Commun 2021;12:961. https://doi.org/10.1038/s41467-021-21213-4.

[7] Wang H, Yang P, Liu K, et al. SARS coronavirus entry into host cells through a novel clathrin- and caveolae-independent endocytic pathway. Cell Res 2008;18:290–301. https://doi.org/10.1038/cr.2008.15.

[8] Yan R, Zhang Y, Li Y, et al. Structural basis for the recognition of SARS-CoV-2 by full-length human ACE2. Science 2020;367:1444–8. https://doi.org/10.1126/science.abb2762.

[9] Monteil V, Kwon H, Prado P, et al. Inhibition of SARS-CoV-2 Infections in Engineered Human Tissues Using Clinical-Grade Soluble Human ACE2. Cell 181 2020:905–913 e907. https://doi.org/10.1016/j.cell.2020.04.004.

[10] Hennighausen L, Lee HK. Activation of the SARS-CoV-2 receptor Ace2 through JAK/STAT-dependent enhancers during pregnancy. Cell Rep 2020;32:. https://doi.org/10.1016/j.celrep.2020.108199108199.

[11] Sandvig K, Kavaliauskiene S, Skotland T. Clathrin-independent endocytosis: an increasing degree of complexity. Histochem Cell Biol 2018;150:107–18. https://doi.org/10.1007/s00418-018-1678-5.

[12] Pelkmans L, Helenius A. Insider information: what viruses tell us about endocytosis. Curr Opin Cell Biol 2003;15:414–22. https://doi.org/10.1016/s0955-0674(03)00081-4.

[13] Cruz-Oliveira C, Freire JM, Conceicao TM, et al. Receptors and routes of dengue virus entry into the host cells. FEMS Microbiol Rev 2015;39:155–70. https://doi.org/10.1093/femsre/fuu004.

[14] Doherty GJ, McMahon HT. Mechanisms of endocytosis. Annu Rev Biochem 2009;78:857–902. https://doi.org/10.1146/annurev.biochem.78.081307.110540.

[15] Anderson HA, Chen Y, Norkin LC. Bound simian virus 40 translocates to caveolin-enriched membrane domains, and its entry is inhibited by drugs that selectively disrupt caveolae. Mol Biol Cell 1996;7:1825–34. https://doi.org/10.1091/mbc.7.11.1825.

[16] Pelkmans L, Puntener D, Helenius A. Local actin polymerization and dynamin recruitment in SV40-induced internalization of caveolae. Science 2002;296:535–9. https://doi.org/10.1126/science.1069784.

[17] Pelkmans L, Kartenbeck J, Helenius A. Caveolar endocytosis of simian virus 40 reveals a new two-step vesicular-transport pathway to the ER. Nat Cell Biol 2001;3:473–83. https://doi.org/10.1038/35074539.

[18] Ewers H, Romer W, Smith AE, et al. GM1 structure determines SV40-induced membrane invagination and infection. Nat Cell Biol 12; 2010: 11-18; sup pp 11-12. https://doi.org/10.1038/ncb1999.

[19] Matveev S, Li X, Everson W, et al. The role of caveolae and caveolin in vesicle-dependent and vesicle-independent trafficking. Adv Drug Deliv Rev 2001;49:237–50. https://doi.org/10.1016/s0169-409x(01)00138-7.

[20] Boucrot E, Ferreira AP, Almeida-Souza L, et al. Endophilin marks and controls a clathrin-independent endocytic pathway. Nature 2015;517:460–5. https://doi.org/10.1038/nature14067.

[21] Chen SL, Liu YG, Zhou YT, et al. Endophilin-A2-mediated endocytic pathway is critical for enterovirus 71 entry into caco-2 cells. Emerg Microbes Infect 2019;8:773–86. https://doi.org/10.1080/22221751.2019.1618686.

[22] Gowrisankaran S, Houy S, Del Castillo JGP, et al. Endophilin-A coordinates priming and fusion of neurosecretory vesicles via intersectin. Nat Commun 2020;11:1266. https://doi.org/10.1038/s41467-020-14993-8.

[23] Renard HF, Simunovic M, Lemiere J, et al. Endophilin-A2 functions in membrane scission in clathrin-independent endocytosis. Nature 2015;517:493–6. https://doi.org/10.1038/nature14064.

[24] Mercer J, Helenius A. Virus entry by macropinocytosis. Nat Cell Biol 2009;11:510–20. https://doi.org/10.1038/ncb0509-510.

[25] Liberali P, Kakkonen E, Turacchio G, et al. The closure of Pak1-dependent macropinosomes requires the phosphorylation of CtBP1/BARS. EMBO J 2008;27:970–81. https://doi.org/10.1038/emboj.2008.59.

[26] Amstutz B, Gastaldelli M, Kalin S, et al. Subversion of CtBP1-controlled macropinocytosis by human adenovirus serotype 3. EMBO J 2008;27:956–69. https://doi.org/10.1038/emboj.2008.38.

[27] Nicola AV, Hou J, Major EO, et al. Herpes simplex virus type 1 enters human epidermal keratinocytes, but not neurons, via a pH-dependent endocytic pathway. J Virol 2005;79:7609–16. https://doi.org/10.1128/JVI.79.12.7609-7616.2005.

[28] Saeed MF, Kolokoltsov AA, Albrecht T, et al. Cellular entry of ebola virus involves uptake by a macropinocytosis-like mechanism and subsequent trafficking through early and late endosomes. PLoS Pathog 2010;6:. https://doi.org/10.1371/journal.ppat.1001110e1001110.

[29] Chazal N, Gerlier D. Virus entry, assembly, budding, and membrane rafts. Microbiol Mol Biol Rev 67; 2003: 226-237, table of contents. https://doi.org/10.1128/mmbr.67.2.226-237.2003.

[30] Manes S, del Real G, Martinez AC. Pathogens: raft hijackers. Nat Rev Immunol 2003;3:557–68. https://doi.org/10.1038/nri1129.

[31] Bavari S, Bosio CM, Wiegand E, et al. Lipid raft microdomains: a gateway for compartmentalized trafficking of Ebola and Marburg viruses. J Exp Med 2002;195:593–602. https://doi.org/10.1084/jem.20011500.

[32] Manie SN, de Breyne S, Vincent S, et al. Measles virus structural components are enriched into lipid raft microdomains: a potential cellular location for virus assembly. J Virol 2000;74:305–11. https://doi.org/10.1128/jvi.74.1.305-311.2000.

[33] Lu YE, Cassese T, Kielian M. The cholesterol requirement for sindbis virus entry and exit and characterization of a spike protein region involved in cholesterol dependence. J Virol 1999;73:4272–8. https://doi.org/10.1128/JVI.73.5.4272-4278.1999.

[34] Lu Y, Liu DX, Tam JP. Lipid rafts are involved in SARS-CoV entry into Vero E6 cells. Biochem Biophys Res Commun 2008;369:344–9. https://doi.org/10.1016/j.bbrc.2008.02.023.

[35] Raff AB, Woodham AW, Raff LM, et al. The evolving field of human papillomavirus receptor research: a review of binding and entry. J Virol 2013;87:6062–72. https://doi.org/10.1128/JVI.00330-13.

[36] Brandenburg B, Lee LY, Lakadamyali M, et al. Imaging poliovirus entry in live cells. PLoS Biol 2007;5:. https://doi.org/10.1371/journal.pbio.0050183e183.

[37] Li Q, Liu Q, Huang W, et al. Current status on the development of pseudoviruses for enveloped viruses. Rev Med Virol 2018;28. https://doi.org/10.1002/rmv.1963.

[38] Wang N, Han S, Liu R, et al. Chloroquine and hydroxychloroquine as ACE2 blockers to inhibit viropexis of 2019-nCoV Spike pseudotyped virus. Phytomedicine 2020;79:. https://doi.org/10.1016/j.phymed.2020.153333153333.

[39] Hosoki K, Chakraborty A, Sur S. Molecular mechanisms and epidemiology of COVID-19 from an allergist's perspective. J Allergy Clin Immunol 2020;146:285–99. https://doi.org/10.1016/j.jaci.2020.05.033.

[40] Wang J, Gou W, Kim DS, et al. Clathrin-mediated endocytosis of alpha-1 antitrypsin is essential for its protective function in islet cell survival. Theranostics 2019;9:3940–51. https://doi.org/10.7150/thno.31647.

[41] Wang LH, Rothberg KG, Anderson RG. Mis-assembly of clathrin lattices on endosomes reveals a regulatory switch for coated pit formation. J Cell Biol 1993;123:1107–17. https://doi.org/10.1083/jcb.123.5.1107.

[42] Macia E, Ehrlich M, Massol R, et al. Dynasore, a cell-permeable inhibitor of dynamin. Dev Cell 2006;10:839–50. https://doi.org/10.1016/j.devcel.2006.04.002.

[43] Harper CB, Popoff MR, McCluskey A, et al. Targeting membrane trafficking in infection prophylaxis: dynamin inhibitors. Trends Cell Biol 2013;23:90–101. https://doi.org/10.1016/j.tcb.2012.10.007.

[44] Saeed MF, Kolokoltsov AA, Freiberg AN, et al. Phosphoinositide-3 kinase-Akt pathway controls cellular entry of Ebola virus. PLoS Pathog 2008;4:. https://doi.org/10.1371/journal.ppat.1000141e1000141.

[45] Wang S, Huang X, Huang Y, et al. Entry of a novel marine DNA virus, Singapore grouper iridovirus, into host cells occurs via clathrin-mediated endocytosis and macropinocytosis in a pH-dependent manner. J Virol 2014;88:13047–63. https://doi.org/10.1128/JVI.01744-14.

[46] Zhu BY, Shang BY, Du Y, et al. A new HDAC inhibitor cinnamoylphenazine shows antitumor activity in association with intensive macropinocytosis. Oncotarget 2017;8:14748–58. https://doi.org/10.18632/oncotarget.14714.

[47] Wang Y, Lu YF, Li CL, et al. Involvement of Rac1 signalling pathway in the development and maintenance of acute inflammatory pain induced by bee venom injection. Br J Pharmacol 2016;173:937–50. https://doi.org/10.1111/bph.13413.

[48] Viaud J, Peterson JR. An allosteric kinase inhibitor binds the p21-activated kinase autoregulatory domain covalently. Mol Cancer Ther 2009;8:2559–65. https://doi.org/10.1158/1535-7163.MCT-09-0102.

[49] Glende J, Schwegmann-Wessels C, Al-Falah M, et al. Importance of cholesterol-rich membrane microdomains in the interaction of the S protein of SARS-coronavirus with the cellular receptor angiotensin-converting enzyme 2. Virology 2008;381:215–21. https://doi.org/10.1016/j.virol.2008.08.026.

[50] Ferreira APA, Boucrot E. Mechanisms of carrier formation during clathrin-independent endocytosis. Trends Cell Biol 2018;28:188–200. https://doi.org/10.1016/j.tcb.2017.11.004.

[51] Sabharanjak S, Sharma P, Parton RG, et al. GPI-anchored proteins are delivered to recycling endosomes via a distinct cdc42-regulated, clathrin-independent pinocytic pathway. Dev Cell 2002;2:411–23. https://doi.org/10.1016/s1534-5807(02)00145-4.

[52] Lundmark R, Doherty GJ, Howes MT, et al. The GTPase-activating protein GRAF1 regulates the CLIC/GEEC endocytic pathway. Curr Biol 2008;18:1802–8. https://doi.org/10.1016/j.cub.2008.10.044.

[53] Kumari S, Mayor S. ARF1 is directly involved in dynamin-independent endocytosis. Nat Cell Biol 2008;10:30–41. https://doi.org/10.1038/ncb1666.

[54] Hong L, Kenney SR, Phillips GK, et al. Characterization of a Cdc42 protein inhibitor and its use as a molecular probe. The Journal of biological chemistry 2013;288:8531–43. https://doi.org/10.1074/jbc.M112.435941.

[55] Hanin G, Shenhar-Tsarfaty S, Yayon N, et al. Competing targets of microRNA-608 affect anxiety and hypertension. Hum Mol Genet 2014;23:4569–80. https://doi.org/10.1093/hmg/ddu170.

[56] Li X, Geng M, Peng Y, et al. Molecular immune pathogenesis and diagnosis of COVID-19. J Pharm Anal 2020;10:102–8. https://doi.org/10.1016/j.jpha.2020.03.001.

[57] Peng Y, Du N, Lei Y, et al. Structures of the SARS-CoV-2 nucleocapsid and their perspectives for drug design. EMBO J. 2020;39:. https://doi.org/10.15252/embj.2020105938 e105938.

[58] Ni L, Ye F, Cheng ML, et al. Detection of SARS-CoV-2-specific humoral and cellular immunity in COVID-19 convalescent individuals. Immunity 2020;52:971–977 e973. https://doi.org/10.1016/j.immuni.2020.04.023.

[59] Zheng Y, Zhuang MW, Han L, et al. Severe acute respiratory syndrome coronavirus 2 (SARS-CoV-2) membrane (M) protein inhibits type I and III interferon production by targeting RIG-I/MDA-5 signaling. Signal Transduct Target Ther 2020;5:299. https://doi.org/10.1038/s41392-020-00438-7.

[60] Mandala VS, McKay MJ, Shcherbakov AA, et al. Structure and drug binding of the SARS-CoV-2 envelope protein transmembrane domain in lipid bilayers. Nat Struct Mol Biol 2020;27:1202–8. https://doi.org/10.1038/s41594-020-00536-8.

[61] Zhou P, Yang XL, Wang XG, et al. A pneumonia outbreak associated with a new coronavirus of probable bat origin (vol 579, pg 270, 2020), Nature 588; 2020: E6-E6. https://doi.org/10.1038/s41586-020-2012-7.

[62] Wang S, Li W, Hui H, et al. Cholesterol 25-Hydroxylase inhibits SARS-CoV-2 and other coronaviruses by depleting membrane cholesterol. EMBO J 2020; e106057. https://doi.org/10.15252/embj.2020106057.

[63] Zang R, Case JB, Yutuc E, et al. Cholesterol 25-hydroxylase suppresses SARS-CoV-2 replication by blocking membrane fusion. PNAS 2020;117:32105–13. https://doi.org/10.1073/pnas.2012197117.

[64] Nie J, Li Q, Wu J, et al. Establishment and validation of a pseudovirus neutralization assay for SARS-CoV-2. Emerg Microbes Infect 2020;9:680–6. https://doi.org/10.1080/22221751.2020.1743767.

[65] Zang R, Gomez Castro MF, McCune BT, et al. TMPRSS2 and TMPRSS4 promote SARS-CoV-2 infection of human small intestinal enterocytes. Sci Immunol 2020;5. https://doi.org/10.1126/sciimmunol.abc3582.

[66] Hoffmann M, Kleine-Weber H, Pohlmann S. A multibasic cleavage site in the spike protein of SARS-CoV-2 is essential for infection of human lung cells. Mol Cell 2020;78:779–784 e775. https://doi.org/10.1016/j.molcel.2020.04.022.

[67] Yuan Y, Cao D, Zhang Y, et al. Cryo-EM structures of MERS-CoV and SARS-CoV spike glycoproteins reveal the dynamic receptor binding domains. Nat Commun 2017;8:15092. https://doi.org/10.1038/ncomms15092.

[68] Song W, Gui M, Wang X, et al. Cryo-EM structure of the SARS coronavirus spike glycoprotein in complex with its host cell receptor ACE2. PLoS Pathog 2018;14:. https://doi.org/10.1371/journal.ppat.1007236 e1007236.

[69] Lan J, Ge J, Yu J, et al. Structure of the SARS-CoV-2 spike receptor-binding domain bound to the ACE2 receptor. Nature 2020;581:215–20. https://doi.org/10.1038/s41586-020-2180-5.

[70] Walls AC, Park YJ, Tortorici MA, et al. Structure, Function, and Antigenicity of the SARS-CoV-2 Spike Glycoprotein. Cell 2020;181:281–292 e286. https://doi.org/10.1016/j.cell.2020.02.058.

[71] Gheblawi M, Wang K, Viveiros A, et al. Angiotensin-converting enzyme 2: SARS-CoV-2 receptor and regulator of the renin-angiotensin system: celebrating the 20th anniversary of the discovery of ACE2. Circ Res 2020;126:1456–74. https://doi.org/10.1161/CIRCRESAHA.120.317015.

[72] Wang M, Cao R, Zhang L, et al. Remdesivir and chloroquine effectively inhibit the recently emerged novel coronavirus (2019-nCoV) in vitro. Cell Res 2020;30:269–71. https://doi.org/10.1038/s41422-020-0282-0.

[73] Hoffmann M, Mosbauer K, Hofmann-Winkler H, et al. Chloroquine does not inhibit infection of human lung cells with SARS-CoV-2. Nature 2020;585:588–90. https://doi.org/10.1038/s41586-020-2575-3.

[74] Mehra MR, Desai SS, Ruschitzka F, et al. RETRACTED: Hydroxychloroquine or chloroquine with or without a macrolide for treatment of COVID-19: a multinational registry analysis. Lancet 2020. https://doi.org/10.1016/S0140-6736(20)31180-6.

[75] Bukrinsky MI, Mukhamedova N, Sviridov D. Lipid rafts and pathogens: the art of deception and exploitation. J Lipid Res 2020;61:601–10. https://doi.org/10.1194/jlr.TR119000391.

[76] Martin JJ, Holguera J, Sanchez-Felipe L, et al. Cholesterol dependence of Newcastle Disease Virus entry. Biochim Biophys Acta, Mol Cell Biol Lipids 1818;2012:753–61. https://doi.org/10.1016/j.bbamem.2011.12.004.

[77] Chang TH, Segovia J, Sabbah A, et al. Cholesterol-rich lipid rafts are required for release of infectious human respiratory syncytial virus particles. Virology 2012;422:205–13. https://doi.org/10.1016/j.virol.2011.10.029.

[78] Nguyen DH, Hildreth JE. Evidence for budding of human immunodeficiency virus type 1 selectively from glycolipid-enriched membrane lipid rafts. J Virol 2000;74:3264–72. https://doi.org/10.1128/jvi.74.7.3264-3272.2000.

[79] Verma DK, Gupta D, Lal SK. Host lipid rafts play a major role in binding and endocytosis of influenza A virus. Viruses 2018;10. https://doi.org/10.3390/v10110650.

[80] Radenkovic D, Chawla S, Pirro M, et al. Cholesterol in relation to COVID-19: should we care about it?. J Clin Med 2020;9. https://doi.org/10.3390/jcm9061909.

[81] Bailly C, Vergoten G. Glycyrrhizin: An alternative drug for the treatment of COVID-19 infection and the associated respiratory syndrome?. Pharmacol Ther 2020;214:. https://doi.org/10.1016/j.pharmthera.2020.107618 107618.

[82] Guo T, Fan Y, Chen M, et al. Cardiovascular Implications of fatal outcomes of patients with coronavirus disease 2019 (COVID-19). JAMA Cardiol 5; 2020: 811–818. https://doi.org/10.1001/jamacardio.2020.1017.

[83] Wu Z, McGoogan JM. Characteristics of and Important Lessons From the Coronavirus Disease 2019 (COVID-19) Outbreak in China: Summary of a Report of 72314 Cases From the Chinese Center for Disease Control and Prevention. JAMA 323; 2020: 1239–1242. https://doi.org/10.1001/jama.2020.2648.

[84] Zhang XJ, Qin JJ, Cheng X, et al. In-hospital use of statins is associated with a reduced risk of mortality among individuals with COVID-19. Cell Metab 2020;32:176–187 e174. https://doi.org/10.1016/j.cmet.2020.06.015.

[85] Rodrigues-Diez RR, Tejera-Munoz A, Marquez-Exposito L, et al. Statins: Could an old friend help in the fight against COVID-19?. Br J Pharmacol 2020. https://doi.org/10.1111/bph.15166.

[86] Nonnenmacher M, Weber T. Adeno-associated virus 2 infection requires endocytosis through the CLIC/GEEC pathway. Cell Host Microbe 2011;10:563–76. https://doi.org/10.1016/j.chom.2011.10.014.